MODELS OF SMALL-SCALE PATCHINESS

Dennis McGillicuddy, Woods Hole Oceanographic Institution, Bigelow 209b, Mail Stop #11, Woods Hole, MA 02543, USA

doi:10.1006/rwos.2001.0405

Introduction

0001 Patchiness is perhaps the most salient characteristic of plankton populations in the ocean. The scale of this heterogeneity spans many orders of magnitude in its spatial extent, ranging from planetary down to microscale (**Figure 1**). It has been argued that patchiness plays a fundamental role in the functioning of marine ecosystems, insofar as the mean conditions may not reflect the environment to which organisms are adapted. For example, the fact that some abundant predators cannot thrive on the mean concentration of their prey in the ocean implies that they are somehow capable of exploiting small-scale patches of prey whose concentrations are much larger than the mean. Understanding the nature of this patchiness is thus one of the major challenges of oceanographic ecology.

0002 The patchiness problem is fundamentally one of physical–biological–chemical interactions. This interconnection arises from three basic sources: (1) ocean currents continually redistribute dissolved and suspended constituents by advection; (2) space–time fluctuations in the flows themselves impact biological and chemical processes; and (3) organisms are capable of directed motion through the water. This tripartite linkage poses a difficult challenge to understanding oceanic ecosystems: differentiation between the three sources of variability requires accurate assessment of property distributions in space and time, in addition to detailed knowledge of organismal repertoires and the processes by which ambient conditions control the rates of biological and chemical reactions.

0003 Various methods of observing the ocean tend to lie parallel to the axes of the space/time domain in which these physical–biological–chemical interactions take place (**Figure 2**). Given that a purely observational approach to the patchiness problem is not tractable with finite resources, the coupling of models with observations offers an alternative which provides a context for synthesis of sparse data with articulations of fundamental principles assumed to govern functionality of the system. In a sense, models can be used to fill the gaps in the space/time domain shown in **Figure 2**, yielding a framework for exploring the controls on spatially and temporally intermittent processes.

0004 The following discussion highlights only a few of the multitude of models which have yielded insight into the dynamics of plankton patchiness. Examples have been chosen to provide a sampling of scales which can be referred to as 'small' – that is, smaller than the planetary scale shown in **Figure 1A**. In addition, the article attempts to furnish some exposure to the diversity of modeling approaches which can be brought to bear on this problem. These range from abstract theoretical models intended to elucidate specific processes, to complex numerical formulations which can be used to actually simulate observed distributions in detail.

Formulation of the Coupled Problem

0005 A general form of the coupled problem can be written as a three-dimensional advection-diffusion-reaction equation for the concentration C_i of any particular organism of interest:

$$\underbrace{\frac{\partial C_i}{\partial t}}_{\text{local rate of change}} + \underbrace{\nabla\cdot(\mathrm{v}C_i)}_{\text{advection}} - \underbrace{\nabla\cdot(K\nabla C_i)}_{\text{diffuion}} = \underbrace{R_i}_{\text{biological sources/sinks}} \qquad [1]$$

where the vector v represents the fluid velocity plus any biologically induced transport through the water (e.g., sinking, swimming), and K the turbulent diffusivity. The advection term is often written simply as $\mathrm{v}\cdot\nabla C_i$ because the ocean is an essentially incompressible fluid (i.e., $\nabla\cdot\mathrm{v}=0$). The 'reaction term' R_i on the right-hand side represents the sources and sinks due to biological activity.

0006 In essence, this model is a quantitative statement of the *conservation of mass* for a scalar variable in a fluid medium. The advective and diffusive terms simply represent the redistribution of material caused by motion. In the absence of any motion, eqn [1] reduces to an ordinary differential equation describing the biological and/or chemical dynamics. The reader is referred to the review by Donaghay and Osborn for a detailed derivation of the advection-diffusion-reaction equation, including explicit

treatment of the Reynolds decomposition for biological and chemical scalars (see Further Reading).

0007 Any number of advection-diffusion-reaction equations can be posed simultaneously to represent a set of interacting state variables C_i in a coupled model. For example, an ecosystem model including nutrients, phytoplankton, and zooplankton (an 'NPZ' model) could be formulated with $C_1 = N, C_2 = P$ and $C_3 = Z$. The biological dynamics linking these three together could include nutrient uptake, primary production, grazing, and remineralization. R_i would then represent not only birth and mortality, but terms which depend on interactions between the several model components.

Growth and Diffusion – the 'KISS' Model

0008 Some of the earliest models used to investigate plankton patchiness dealt with the competing effects of growth and diffusion. In the early 1950s, models developed independently by Kierstead (KI) and Slobodkin (S) and Skellam (S) – the so-called 'KISS' model – were formulated as a one-dimensional diffusion equation with exponential population growth and constant diffusivity:

$$\frac{\partial C}{\partial t} - K\frac{\partial^2 C}{\partial x^2} = \alpha C \qquad [2]$$

Note that this model is a reduced form of eqn [1]. It is a mathematical statement that the tendency for organisms to accumulate through reproduction is counterbalanced by the tendency of the environment to disperse them through turbulent diffusion. Seeking solutions which vanish at $x = 0$ and $x = L$ (thereby defining a characteristic patch size of dimension L), with initial concentration $C(x, 0) = f(x)$, one can solve for a critical patch size $L = \pi(K/\alpha)^{\frac{1}{2}}$ in which growth and dispersal are in perfect balance. For a specified growth rate α and diffusivity K, patches smaller than L will be eliminated by diffusion, while those that are larger will result in blooms. Although highly idealized in its treatment of both physical transport and biological dynamics, this model illuminates a very important aspect of the role of diffusion in plankton patchiness. In addition, it led to a very specific theoretical prediction of the initial conditions required to start a plankton bloom, which Slobodkin subsequently applied to the problem of harmful algal blooms on the west Florida shelf.

Homogeneous Isotropic Turbulence

The physical regime to which the preceding model best applies is one in which the statistics of the turbulence responsible for diffusive transport is spatially uniform (*homogeneous*) and has no preferred direction (*isotropic*). Turbulence of this type may occur locally in parts of the ocean in circumstances where active mixing is taking place, such as in a wind-driven surface mixing layer. Such motions might produce plankton distributions such as those shown in **Figure 1E**. 0009

The nature of homogeneous isotropic turbulence was characterized by Kolmogoroff in the early 1940s. He suggested that the scale of the largest eddies in the flow was set by the nature of the external forcing. These large eddies transfer energy to smaller eddies down through the *inertial subrange* in what is known as the turbulent cascade. This cascade continues to the Kolmogoroff microscale, at which viscous forces dissipate the energy into heat. This elegant physical model inspired the following poem attributed to L.F. Richardson: 0010

Big whorls make little whorls
which feed on their velocity;
little whorls make smaller whorls,
and so on to viscosity...

Based on dimensional considerations, Kolmogoroff proposed an energy spectrum E of the form 0011

$$E(k) = A\varepsilon^{\frac{2}{3}}k^{-\frac{5}{3}}$$

where k is the wavenumber, ε is the dissipation rate of turbulent kinetic energy, and A is a dimensionless constant. This theoretical prediction was later borne out by measurements, which confirmed the 'minus five-thirds' dependence of energy content on wavenumber.

In the early 1970s, Platt published a startling set of measurements which suggested that for scales between 10 and 10^3 m the variance spectrum of chlorophyll in the Gulf of St Lawrence showed the same $-5/3$ slope. On the basis of this similarity to the Kolmogoroff spectrum, he argued that on these scales, phytoplankton were simply passive tracers of the turbulent motions. These findings led to a burgeoning field of spectral modeling and analysis of plankton patchiness. Studies by Denman, Powell, Fasham, and others sought to formulate more unified theories of physical–biological interactions using this general approach. For example, Denman and Platt extended a model for the scalar variance 0012

spectrum to include a uniform growth rate. Their theoretical analysis suggested a breakpoint in the spectrum at a critical wavenumber k_c (**Figure 3**), which they estimated to be in the order of $1\,km^{-1}$ in the upper ocean. For wavenumbers lower than k_c, phytoplankton growth tends to dominate the effects of turbulent diffusion, resulting in a k^{-1} dependence. In the higher wavenumber region, turbulent motions overcome biological effects, leading to spectral slopes of -2 to -3. Efforts to include more biological realism in theories of this type have continued to produce interesting results, although Powell and others have cautioned that spectral characteristics may not be sufficient in and of themselves to resolve the underlying physical–biological interactions controlling plankton patchiness in the ocean.

Vertical Structure

0013 Perhaps the most ubiquitous aspect of plankton distributions which makes them *anisotropic* is their vertical structure. Organisms stratify themselves in a multitude of ways, for any number of different purposes (e.g., to exploit a limiting resource, to avoid predation, to facilitate reproduction). For example, consider the subsurface maximum which is characteristic of the chlorophyll distribution in many parts of the world ocean (**Figure 4**) The deep chlorophyll maximum (DCM) is typically situated below the nutrient-depleted surface layer, where nutrient concentrations begin to increase with depth. Generally this is interpreted to be the result of joint resource limitation: the DCM resides where nutrients are abundant and there is sufficient light for photosynthesis. However, this maximum in chlorophyll does not necessarily imply a maximum in phytoplankton biomass. For example, in the nutrient-impoverished surface waters of the open ocean, much of the phytoplankton standing stock is sustained by nutrients which are rapidly recycled; thus relatively high biomass is maintained by low ambient nutrient concentrations. In such situations, the DCM often turns out to be a pigment maximum, but not a biomass maximum. The mechanism responsible for the DCM in this case is *photoadaptation*, the process by which phytoplankton alter their pigment content according to the ambient light environment. By manufacturing more chlorophyll per cell, phytoplankton populations in this type of DCM are able to capture photons more effectively in a low-light environment.

0014 Models have been developed which can produce both aspects of the DCM. For example, consider the nutrient, phytoplankton, zooplankton, detritus (NPZD) type of model (**Figure 5**) which simulates the flows of nitrogen in a planktonic ecosystem. The various biological transformations (such as nutrient uptake, primary production, grazing excretion, etc.) are represented mathematically by functional relationships which depend on the model state variables and parameters which must be determined empirically. Doney *et al.* coupled such a system to a one-dimensional physical model of the upper ocean (**Figure 6**). Essentially, the vertical velocity (w) and diffusivity fields from the physical model are used to drive a set of four coupled advection-diffusion-reaction equations (one for each ecosystem state variable) which represent a subset of the full three-dimensional eqn [1]:

$$\frac{\partial C_i}{\partial t} + w\frac{\partial C_i}{\partial z} - \frac{\partial}{\partial z}\left(K\frac{\partial C_i}{\partial z}\right) = R_i \qquad [3]$$

The R_i terms represent the ecosystem interaction terms schematized in **Figure 5**. Using a diagnostic photoadaptive relationship to predict chlorophyll from phytoplankton nitrogen and the ambient light and nutrient fields, such a model captures the overall character of the DCM observed at the Bermuda Atlantic Time-series Study (BATS) site (**Figure 6**).

Broad-scale vertical patchiness (on the scale of the seasonal thermocline) such as the DCM is accompanied by much finer structure. The special volume of *Oceanography* on 'Thin layers' provides an excellent overview of this subject, documenting small-scale vertical structure in planktonic populations of many different types. One particularly striking example comes from high-resolution fluorescence measurements (**Figure 7A**). Such profiles often show strong peaks in very narrow depth intervals, which presumably result from thin layers of phytoplankton. A mechanism for the production of this layering was identified in a modeling study by P.J.S. Franks, in which he investigated the impact of near-inertial wave motion on the ambient horizontal and vertical patchiness which exists at scales much larger than the thin layers of interest. Near-inertial waves are a particularly energetic component in the internal wave spectrum of the ocean. Their horizontal velocities can be described by:

$$u = U_0\cos(mz - \omega t) \quad v = U_0\sin(mz - \omega t) \qquad [4]$$

where U_0 is a characteristic velocity scale, m is the vertical wavenumber, and ω the frequency of the wave. This kinematic model prescribes that the velocity vector rotates clockwise in time and counterclockwise with depth; its phase velocity is downward, and group velocity upward. In his

words, 'the motion is similar to a stack of pancakes, each rotating in its own plane, and each slightly out of phase with the one below'. Franks used this velocity field to perturb an initial distribution of phytoplankton in which a Gaussian vertical distribution (of scale σ) varied sinusoidally in both x and y directions with wavenumber k_P. Neglecting the effects of growth and mixing, and assuming that phytoplankton are advected passively with the flow, eqn [1] reduces to:

$$\frac{\partial C}{\partial t} + u\frac{\partial C}{\partial x} + v\frac{\partial C}{\partial y} = 0 \qquad [5]$$

Plugging the velocity fields [4] into this equation, the initial phytoplankton distribution can be integrated forward in time. This model demonstrates the striking result that such motions can generate vertical structure which is much finer than that present in the initial condition (**Figure 7B**). Analysis of the simulations revealed that the mechanism at work here is simple and elegant: vertical shear can translate horizontal patchiness into thin layers by stretching and tilting the initial patch onto its side (**Figure 7C**).

Mesoscale Processes: The Internal Weather of the Sea

0016 Just as the atmosphere has weather patterns that profoundly affect the plants and animals that live on the surface of the earth, the ocean also has its own set of environmental fluctuations which exert fundamental control over the organisms living within it. The currents, fronts, and eddies that comprise the oceanic mesoscale, sometimes referred to as the 'internal weather of the sea', are highly energetic features of ocean circulation. Driven both directly and indirectly by wind and buoyancy forcing, their characteristic scales range from tens to hundreds of kilometers with durations of weeks to months. Their space scales are thus smaller and timescales longer than their counterparts in atmospheric weather, but the dynamics of the two systems are in many ways analogous. Impacts of these motions on surface ocean chlorophyll distributions are clearly visible in satellite imagery (**Figure 1B**).

0017 Mesoscale phenomenologies accommodate a diverse set of physical–biological interactions which influence the distribution and variability of plankton populations in the sea. These complex yet highly organized flows continually deform and rearrange the hydrographic structure of the near-surface region in which plankton reside. In the most general terms, the impact of these motions on the biota is twofold: not only do they stir organism distributions, they can also modulate the rates of biological processes. Common manifestations of the latter are associated with vertical transports which can affect the availability of both nutrients and light to phytoplankton, and thereby the rate of primary production. The dynamics of mesoscale and submesoscale flows are replete with mechanisms that can produce vertical motions.

0018 Some of the first investigations of these effects focused on mesoscale jets. Their internal mechanics are such that changes in curvature give rise to horizontal divergences which lead to very intense vertical velocities along the flanks of the meander systems (**Figure 8**). J.D. Woods was one of the first to suggest that these submesoscale upwellings and downwellings would have a strong impact on upper ocean plankton distributions (see his article contained in the volume edited by Rothschild; see Further Reading). Subsequent modeling studies have investigated these effects by incorporating planktonic ecosystems of the type shown in **Figure 5** into three-dimensional dynamical models of meandering jets. Results suggest that upwelling in the flank of a meander can stimulate the growth of phytoplankton (**Figure 9**). Simulated plankton fields are quite complex owing to the fact that fluid parcels are rapidly advected in between regions of upwelling and downwelling. Clearly, this complicated convolution of physical transport and biological response can generate strong heterogeneity in plankton distributions.

0019 What are the implications of mesoscale patchiness? Do these fluctuations average out to zero, or are they important in determining the mean characteristics of the system? In the Sargasso Sea, it appears that mesoscale eddies are a primary mechanism by which nutrients are transported to the upper ocean. Numerical simulations were used to suggest that upwelling due to eddy formation and intensification causes intermittent fluxes of nitrate into the euphotic zone (**Figure 10A**). The mechanism can be conceptualized by considering a density surface with mean depth coincident with the base of the euphotic zone (**Figure 10B**). This surface is perturbed vertically by the formation, evolution, and destruction of mesoscale features. Shoaling density surfaces lift nutrients into the euphotic zone which are rapidly utilized by the biota. Deepening density surfaces serve to push nutrient-depleted water out of the well-illuminated surface layers. The asymmetric light field thus rectifies vertical displacements of both directions into a net upward transport of nutrients, which is presumably balanced by a commen-

surate flux of sinking particulate material. Several different lines of evidence suggest that eddy-driven nutrient flux represents a large portion of the annual nitrogen budget in the Sargasso Sea. Thus, in this instance, plankton patchiness appears to be an essential characteristic which drives the mean properties of the system.

Coastal Processes

0020 Of course, the internal weather of the sea is not limited to the eddies and jets of the open ocean. Coastal regions contain a similar set of phenomena, in addition to a suite of processes in which the presence of a land boundary plays a key role. A canonical example of such a process is coastal upwelling, in which the surface layer is forced offshore when the wind blows from a particular direction. This triggers upwelling of deep water to replace the displaced surface water. The biological ramifications of this were explored in the mid-1970s by Wroblewski with one of the first coupled physical–biological models to include spatial variability explicitly. Configuring a two-dimensional advection-diffusion-reaction model in vertical plane cutting across the Oregon shelf, he studied the response of an NPZD-type ecosystem model to transient wind forcing. His 'strong upwelling' case provided a dramatic demonstration of mesoscale patch formation (**Figure 11**). Deep, nutrient-rich waters from the bottom boundary layer drawn up toward the surface stimulate a large increase in primary production which is restricted to within 10 km of the coast. The phytoplankton distribution reflects the localized enhancement of production, in addition to advective transport of the resultant biogenic material. Note that the highest concentrations of phytoplankton are displaced from the peak in primary production, owing to the offshore transport in the near-surface layers.

0021 Although Wroblewski's model was able to capture some of the most basic elements of the biological response to coastal upwelling, its two-dimensional formulation precluded representation of alongshore variations which can sometimes be as dramatic as those in the cross-shore direction. The complex set of interacting jets, eddies, and filaments characteristic of such environments (as in **Figure 1C**) have been the subject of a number of three-dimensional modeling investigations. For example, Moisan *et al*. incorporated a food web and bio-optical model into simulations of the Coastal Transition Zone off California. This model showed how coastal filaments can produce a complex biological response through modulation of the ambient light and nutrient fields (**Figure 12**). The simulations suggested that significant cross-shelf transport of carbon can occur in episodic pulses when filaments meander offshore. These dynamics illustrate the tremendous complexity of the processes which link the coastal ocean with the deep sea.

Behavior

The mechanisms for generating plankton patchiness described thus far consist of some combination of fluid transport and physiological response to the physical, biological, and chemical environment. The fact that many planktonic organisms have behavior (interpreted narrowly here as the capability for directed motion *through* the water) facilitates a diverse array of processes for creating heterogeneity in their distributions. Such processes pose particularly difficult challenges for modeling, in that their effects are most observable at the level of the *population*, whereas their dynamics are governed by interactions which occur amongst *individuals*. The latter aspect makes modeling patchiness of this type particularly amenable to individual-based models, in contrast to the concentration-based model described by eqn [1]. For example, many species of marine plankton are known to form dense aggregations, sometimes referred to as swarms. Okubo suggested an individual-based model for the maintenance of a swarm of the form: 0022

$$\frac{d^2x}{dt^2} = -k\frac{dx}{dt} - \omega^2 x - \phi(x) + A(t) \qquad [6]$$

where x represents the position of an individual. This model assumes a frictional force on the organism which is proportional to its velocity (with frictional coefficient k), a random force $A(t)$ which is white noise of zero mean and variance B, and attractive forces. Acceleration resulting from the attractive forces is split between periodic (frequency ω) and static ($\phi(x)$) components. The key aspect of the attractive forces is that they depend on the distance from the center of the patch. A Fokker-Planck equation can be used to derive a probability density function:

$$p(x) = p_0 \exp\left(-\frac{\omega^2}{2B}x^2 - \int \frac{\phi(x)}{b}\, dx \right) \qquad [7]$$

where p_0 is the density at the center of the swarm. Thus, the macroscopic properties of the system can be related to the specific set of rules governing individual behavior. Okubo has shown that ob-

served characteristics of insect swarms compare well with theoretical predictions from this model, both in terms of the organism velocity autocorrelation and the frequency distribution of their speeds. Analogous comparisons with plankton have proven elusive owing to the extreme difficulty in making such measurements in marine systems.

0023 The foregoing example illustrates how swarms can arise out of purely behavioral motion. Yet another class of patchiness stems from the joint effects of behavior and fluid transport. The paper by Flierl *et al.* is an excellent reference on this general topic (see Further Reading). One of the simplest examples of this kind of process arises in a population which is capable of maintaining its depth (either through swimming or buoyancy effects) in the presence of convergent flow. With no biological sources or sinks, eqn [1] becomes:

$$\frac{\partial C}{\partial t} + \mathrm{v}\cdot\nabla_H C + C\nabla_H\cdot\mathrm{v} - \nabla\cdot(K\nabla C_i) = 0 \qquad [8]$$

where ∇_H is the vector derivative in the horizontal direction only. Because vertical fluid motion is exactly compensated by organism behavior (recall that the vector **v** represents the sum of physical and biological velocities), two advective contributions arise from the term $\nabla\cdot(\mathrm{v}C)$ in eqn [1]: the common form with the horizontal velocity operating on spatial gradients in concentration, *plus* a source/sink term created by the divergence in total velocity (fluid + organism). The latter term provides a mechanism for accumulation of depth-keeping organisms in areas of fluid convergence. It has been suggested that this process is important in a variety of different oceanic contexts. In the mid-1980s, Olson and Backus argued it could result in a 100-fold increase in the local abundance of a mesopelagic fish *Benthosema glaciale* in a warm core ring. Franks modeled a conceptually similar process with a surface-seeking organism in the vicinity of a propagating front (**Figure 13**). Simply stated, upward swimming organisms tend to accumulate in areas of downwelling. This mechanism has been suggested to explain spectacular accumulations of motile dinoflagellates at fronts (**Figure 1D**).

Conclusions

0024 The interaction of planktonic population dynamics with oceanic circulation can create tremendously complex patterns in the distribution of organisms. Even an ocean at rest could accommodate significant inhomogeneity through geographic variations in environmental variables, time-dependent forcing, and organism behavior. Fluid motions tend to amalgamate all of these effects in addition to introducing yet another source of variability: space–time fluctuations in the flows themselves which impact biological processes. Understanding the mechanisms responsible for observed variations in plankton distributions is thus an extremely difficult task.

Coupled physical–biological models offer a framework for dissection of these manifold contributions to structure in planktonic populations. Such models take many forms in the variety of approaches which have been used to study plankton patchiness. In theoretical investigations, the basic dynamics of idealized systems are worked out using techniques from applied mathematics and mathematical physics. Process-oriented numerical models offer a conceptually similar way to study systems that are too complex to be solved analytically. Simulation-oriented models are aimed at reconstructing particular data sets using realistic hydrodynamic forcing pertaining to the space/time domain of interest. Generally speaking, such models tend to be quite complex because of the multitude of processes which must be included to simulate observations made in the natural environment. Of course, this complexity makes diagnosis of the coupled system more challenging. Nevertheless, the combination of models and observations provides a unique context for the synthesis of necessarily sparse data: space–time continuous representations of the real ocean which can be diagnosed term-by-term to reveal the underlying processes. Formal union between models and observations is beginning to occur through the emergence of inverse methods and data assimilation in the field of biological oceanography. Article no. ● ● ● provides an up-to-date review of this very exciting and rapidly evolving aspect of coupled physical–biological modeling. 0025

Although the field is more than a half-century old, modeling of plankton patchiness is still in its infancy. The oceanic environment is replete with phenomena of this type which are not yet understood. Fortunately, the field is perhaps better poised than ever to address such problems. Recent advances in measurement technologies (e.g., high-resolution acoustical and optical methods, miniaturized biological and chemical sensors) are beginning to provide direct observations of plankton on the scales at which the coupled processes operate. Linkage of such measurements with models is likely to yield important new insights into the mechanisms controlling plankton patchiness in the ocean. 0026

See also

0027 **Biogeochemical Data Assimilation (410). Coastal Circulation Models (400). Fish Vertical Migration (20). Fishery Management (459). Fossil Turbulence (138). General Processes in Ocean Circulation (107). Patch Dynamics (290). 205. 346.**

Further Reading

Denman KL and Gargett AE (1995) Biological–physical interactions in the upper ocean: the role of vertical and small scale transport processes. *Annual Reviews of Fluid Mechanics* 27: 225–255.

Donaghay PL and Osborn TR (1997) Toward a theory of biological–physical control on harmful algal bloom dynamics and impacts. *Limnology and Oceanography* 42: 1283–1296.

Flierl GR, Grunbaum D, Levin S and Olson DB (1999) From individuals to aggregations: the interplay between behavior and physics. *Journal of Theoretical Biology* 196: 397–454.

Franks PJS (1995) Coupled physical–biological models in oceanography. *Reviews of Geophysics* (supplement): 1177–1187.

Franks PJS (1997) Spatial patterns in dense algal blooms. *Limnology and Oceanography* 42: 1297–1305.

Levin S, Powell TM and Steele JH (1993) *Patch Dynamics*. Berlin: Springer-Verlag.

Mackas DL, Denman KL and Abbott MR (1985) Plankton patchiness: biology in the physical vernacular. *Bulletin of Marine Science* 37: 652–674.

Mann KH and Lazier JRN (1996) *Dynamics of Marine Ecosystems: Biological–Physical Interactions in the Oceans*. Oxford: Blackwell Scientific Publications.

Okubo A (1980) *Diffusion and Ecological Problems*: Mathematical Models. Berlin: Springer-Verlag.

Okubo A (1986) Dynamical aspects of animal grouping: swarms, schools, flocks and herds. *Advances in Biophysics* 22: 1–94.

Robinson AR, McCarthy JJ and Rothschild BJ (2001) *The Sea: Biological–physical Interactions in the Ocean*. New York: John Wiley and Sons.

Rothschild BJ (1988) *Toward a Theory on Biological–Physical Interactions in the World Ocean*. Dordrecht: D. Reidel.

Oceanography Society (1998) *Oceanography* 11(1): *Special Issue on Thin Layers*. Virginia Beach, VA: Oceanography Society.

Steele JH (1978) *Spatial Pattern in Plankton Communities*. New York: Plenum Press.

Wroblewski JS and Hofmann EE (1989) U.S. interdisciplinary modeling studies of coastal-offshore exchange processes: past and future. *Progress in Oceanography* 23: 65–99.

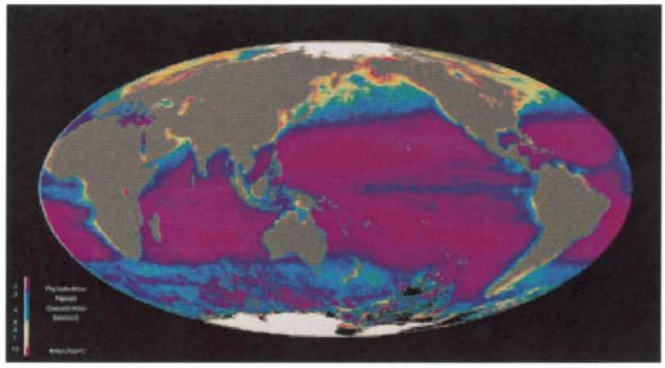

(A)

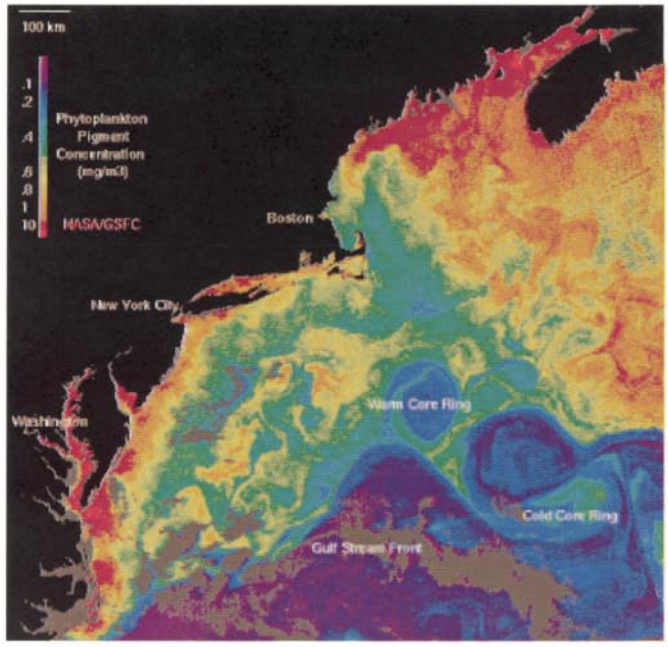

(B)

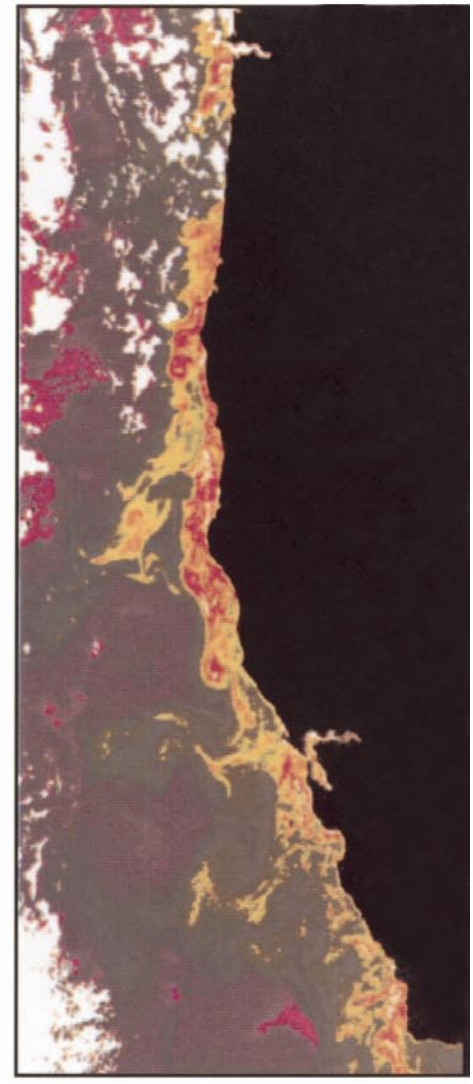

(C)

(D)

(E)

0405f 0001

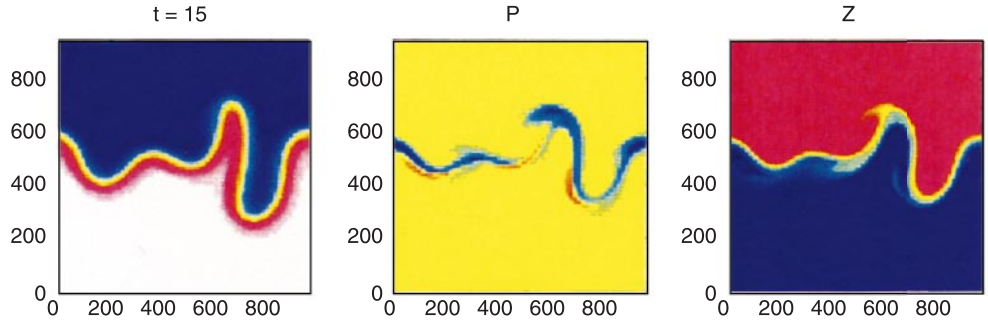

a0405fig0009 **Figure 9** Results from a coupled model of the Gulf Stream: thermocline depth (left), phytoplankton concentration (middle), and zooplankton concentration (right). (From Flierl and McGillicuddy, submitted.)

Figure 1 Appears on Previous Page

Figure 1 Scales of plankton patchiness, ranging from global down to 1 cm. (A-C) satellite-based estimates of surface-layer chlorophyll computed from ocean color measurements. (D) A dense stripe of *Noctiluca scintillans*, 3 km off the coast of La Jolla. The boat in the photograph is trailing a line with floats spaced every 20 m. The stripe stretched for at least 20 km parallel to the shore (photograph courtesy of P.J.S. Franks). (E) Surface view of a bloom of *Anabaena flos-aquae* in Malham Tarn, Scotland. The area shown is approximately 1 m^2 (photograph courtesy of G.E. Fogg).

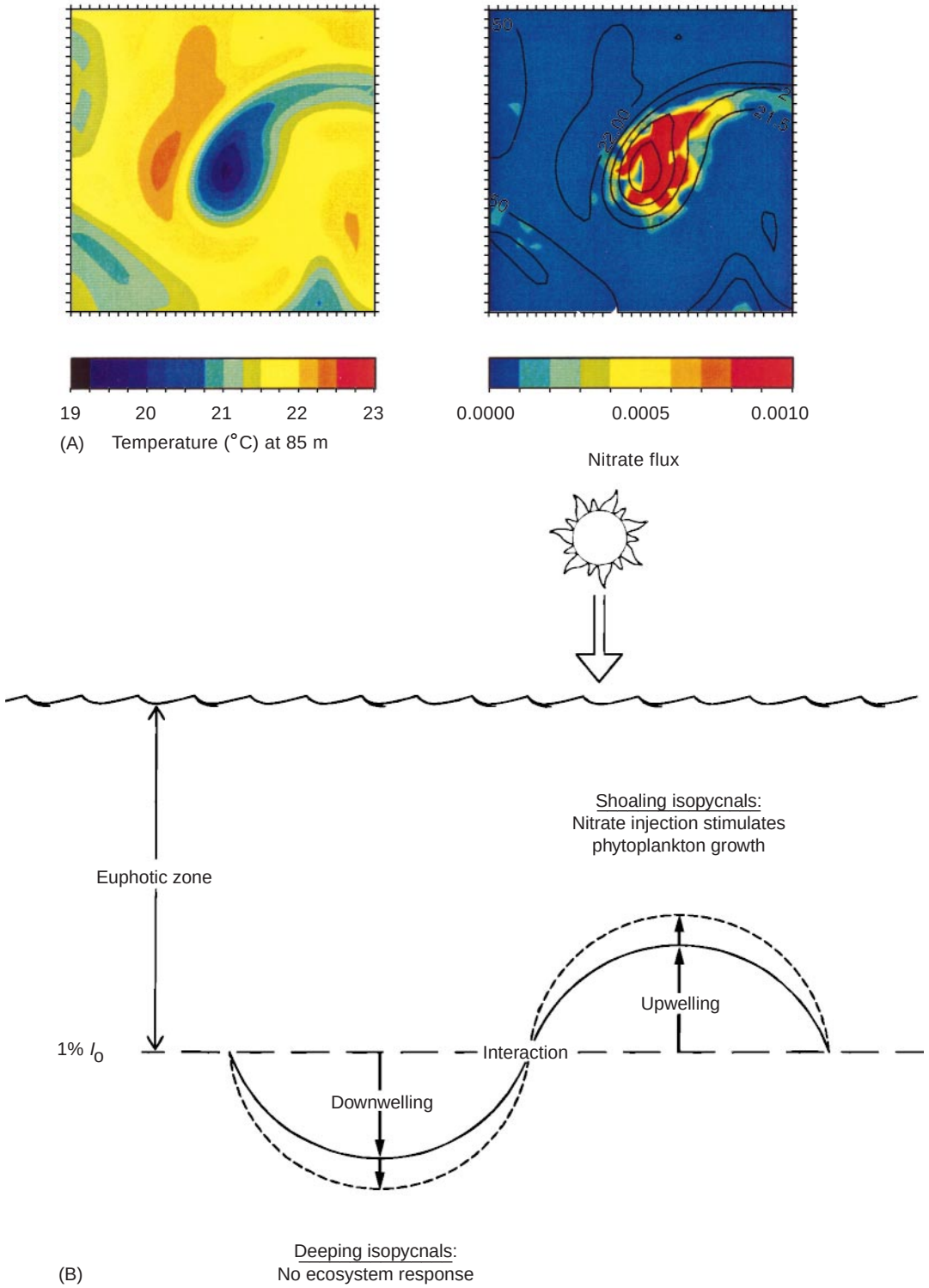

a0405fig0010 **Figure 10** (A) A simulated eddy-driven nutrient injection event: snapshots of temperature at 85 m (left column, °C) and nitrate flux across the base of the euphotic zone (right column, moles of nitrogen $m^2 d^{-1}$). For convenience, temperature contours from the left-hand panels are overlayed on the nutrient flux distributions. The area shown here is a 500 km^2 domain. (The simulation is described in McGillicuddy DJ and Robinson AR (1997) Eddy induced nutrient supply and new production in the Sargasso Sea. *Deep-Sea Research I* 44(8): 1427–1450.) (B) A schematic representation of the eddy upwelling mechanism. The solid line depicts the vertical deflection of an individual isopycnal caused by the presence of two adjacent eddies of opposite sign. The dashed line indicates how the isopycnal might be subsequently perturbed by interaction of the two eddies. (Reproduced with permission from McGillicuddy DJ, Robinson AR, Siegel *et al.* (1998) Influence of mesoscale eddies on new production in the Sargasso Sea. *Nature* 394: 263–265.

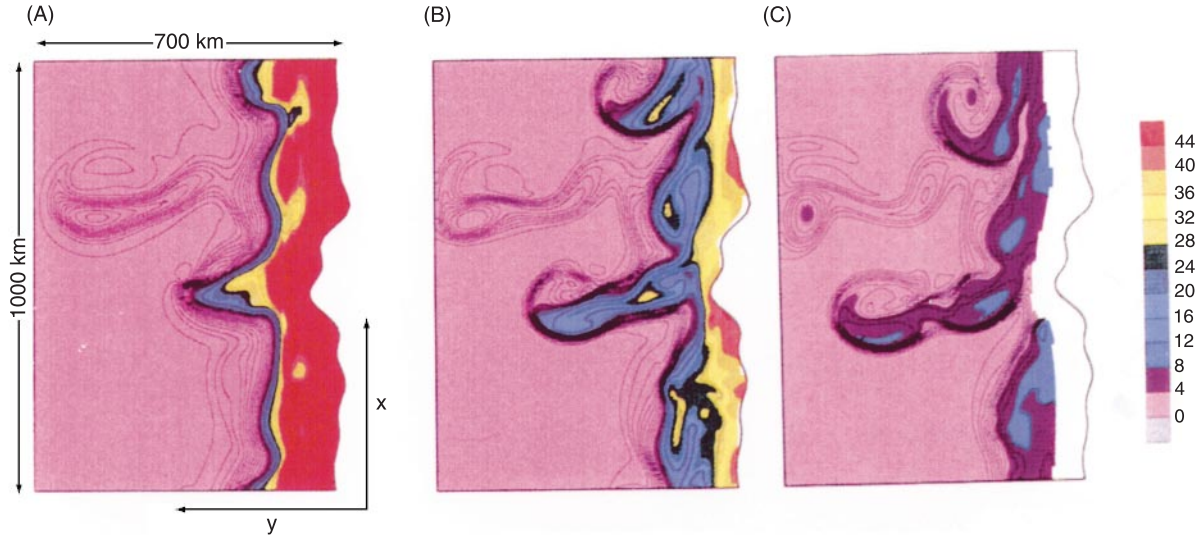

a0405fig0012 **Figure 12** Modeled distributions of phytoplankton (color shading, mg nitrogen m^{-3}) in the Coastal Transition Zone off California. Instantaneous snapshots in panels (A–C) are separated by time intervals of 10 days. Contour lines indicate the depth of the euphotic zone, defined as the depth at which photosynthetically available radiation is 1% of its value at the surface. Contours range from 30 to 180 m, 40 to 180 m, and 60 to 180 m in panels (A), (B), and (C) respectively. (Reproduced with permission from Moisan *et al.* (1996) Modeling nutrient and plankton processes in the California coastal transition zone 2. A three-dimensional physical-bio-optical model. *Journal of Geophysical Research* 101(C10): 22 677–22 691.

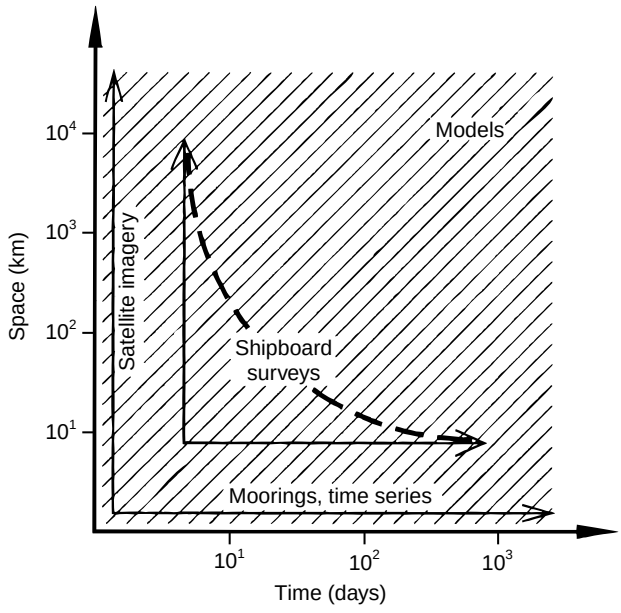

a0405fig0002 **Figure 2** Space–time diagram of the scales resolvable with current observational capabilities. Measurements tend to fall along the axes; the dashed line running between the 'shipboard survey' axes reflects the trade-off between spatial coverage and temporal resolution inherent in seagoing operations of that type. Models can be used to examine portions of the space–time continuum (shaded area).

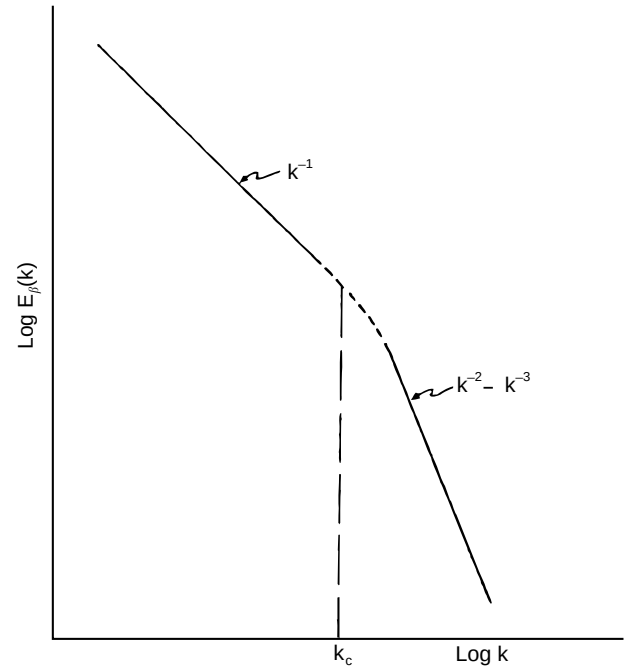

Figure 3 A theoretical spectrum for the spatial variability of phytoplankton, $E_\beta(k)$, as a function of wavenumber, k, displayed on a log-log plot. To the left of the critical wavenumber k_c, biological processes dominate, resulting in a k^{-1} dependence. The high wavenumber region to the right of k_c where turbulent motions dominate, has a dependence. The high wavenumber region to the right of k_c where turbulent motionsdominate, has a dependence between k^{-2} and k^{-3}. (Reproduced with permission from Denman and Platt (1976). The variance spectrum of phytoplankton in a turbulent ocean. *Journal of Marine Research* 34: 593–601.) a0405fig0003

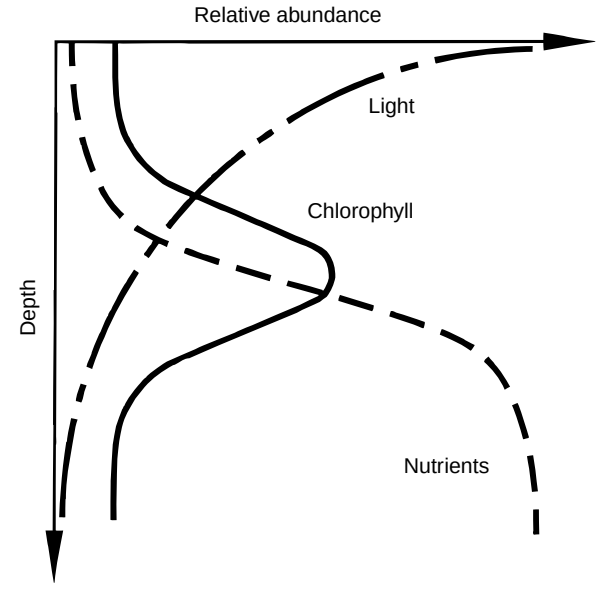

Figure 4 Schematic representation of the deep chlorophyll maximum in relation to ambient light and nutrient profiles. a0405fig0004

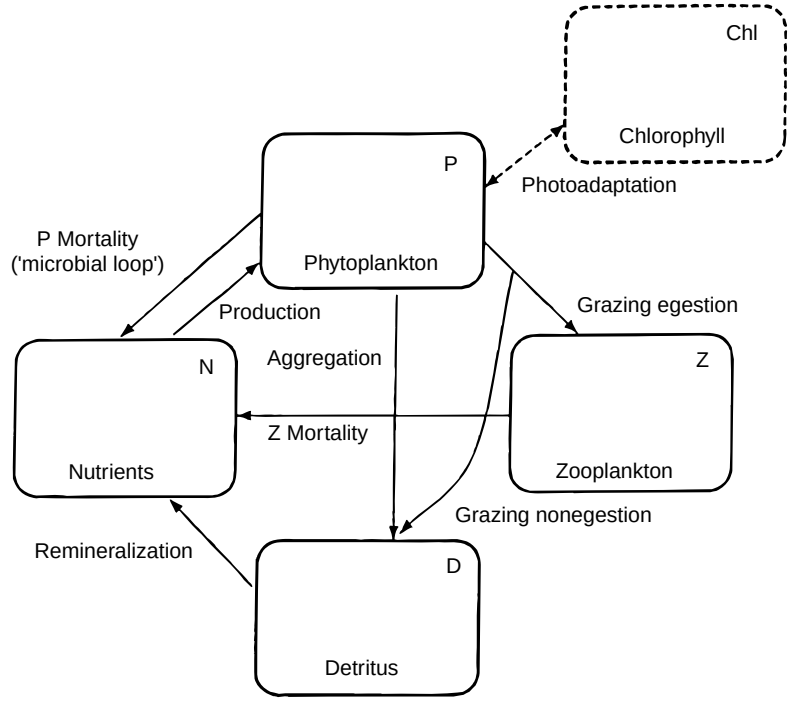

a0405fig0005 **Figure 5** A four-compartment planktonic ecosystem model showing the pathways for nitrogen flow. (Reproduced with permission from Doney SC, Glover DM and Najjar RG (1996) A new coupled, one-dimensional biological–physical model for the upper ocean: applications to the JGOFS Bermuda Atlantic Time-series Study (BATS) site. *Deep-Sea Research II* 43: 591–624.)

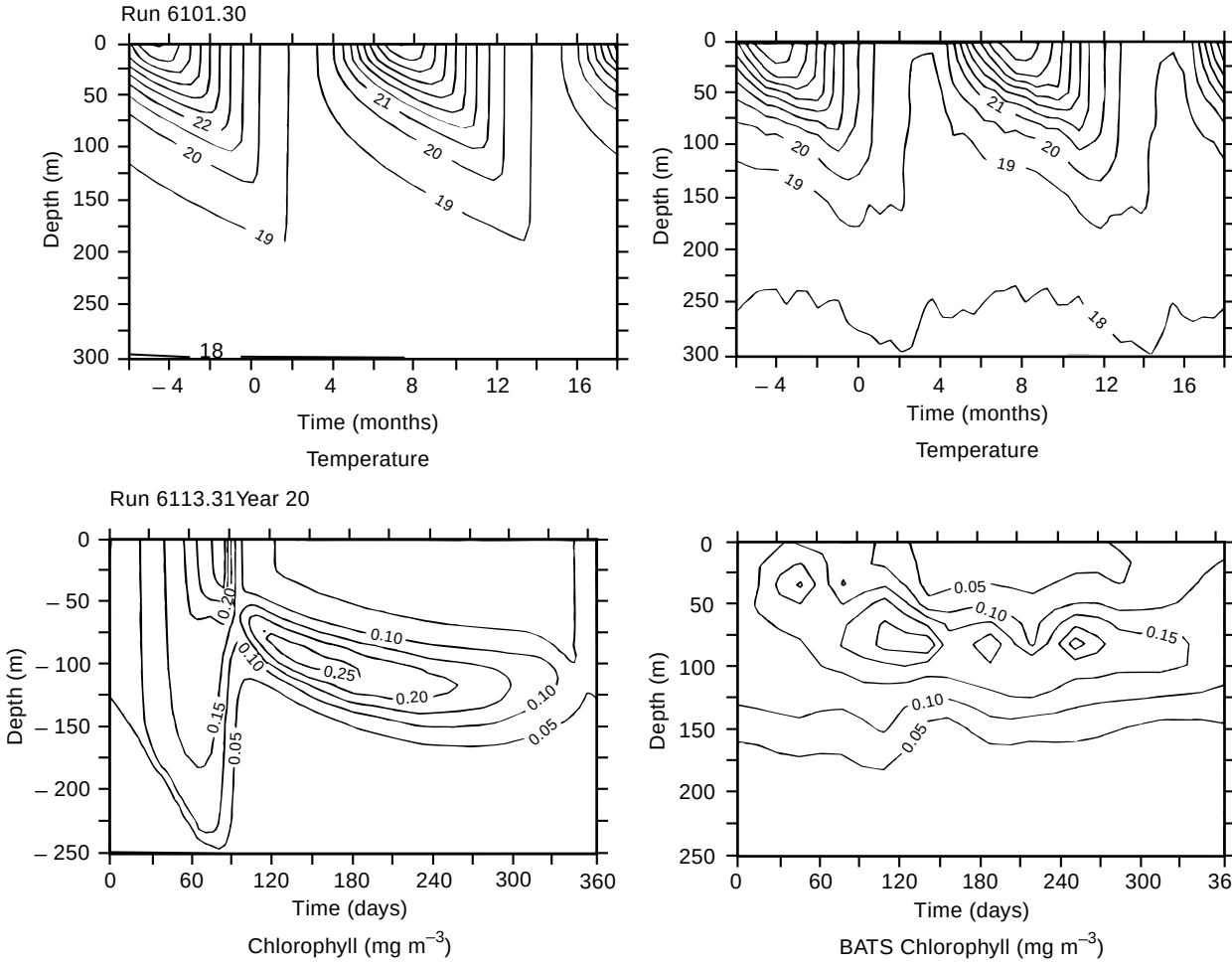

a0405fig0006 **Figure 6** Simulated (left) and observed (right) seasonal cycles of temperature and chlorophyll at the BATS site. (Reproduced with permission from Doney SC, Glover DM and Najjar RG (1996) A new coupled, one-dimensional biological–physical model for the upper ocean: applications to the JGOFS Bermuda Atlantic Time-series Study (BATS) site. *Deep-Sea Research II* 43: 591–624.)

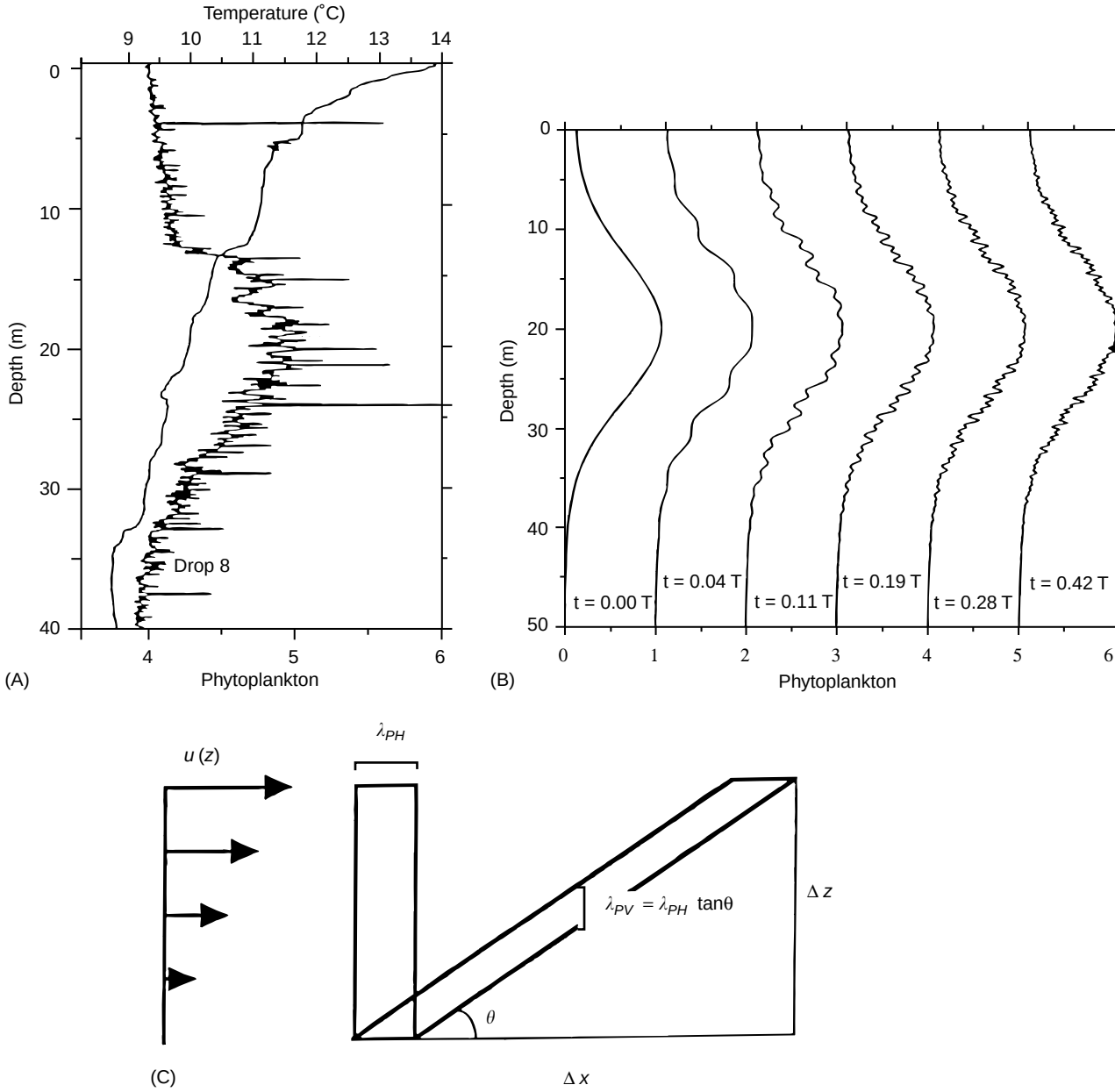

a0405fig0007 **Figure 7** (A) Observations of thin layer structure in a high-resolution profile of fluorescence (thick line, arbitrary units). The thin line shows the corresponding temperature structure. (Data courtesy of Dr T. Cowles.) (B) Simulated vertical profiles of phytoplankton concentration (arbitrary units) as six sequential times. Each profile is offset from the previous by 1 phytoplankton unit. The times are given as fractions of the period of the near-inertial wave used to drive the model. (C) A schematic diagram of the layering process. Vertical shear stretches a vertical column of a property horizontally through an angle θ, creating a layer in the vertical profile. (Reproduced with permission from Franks PJS (1995) Thin layers of phytoplankton: a model of formation by near-inertial wave shear. *Deep-Sea Research I* 42: 75–91.

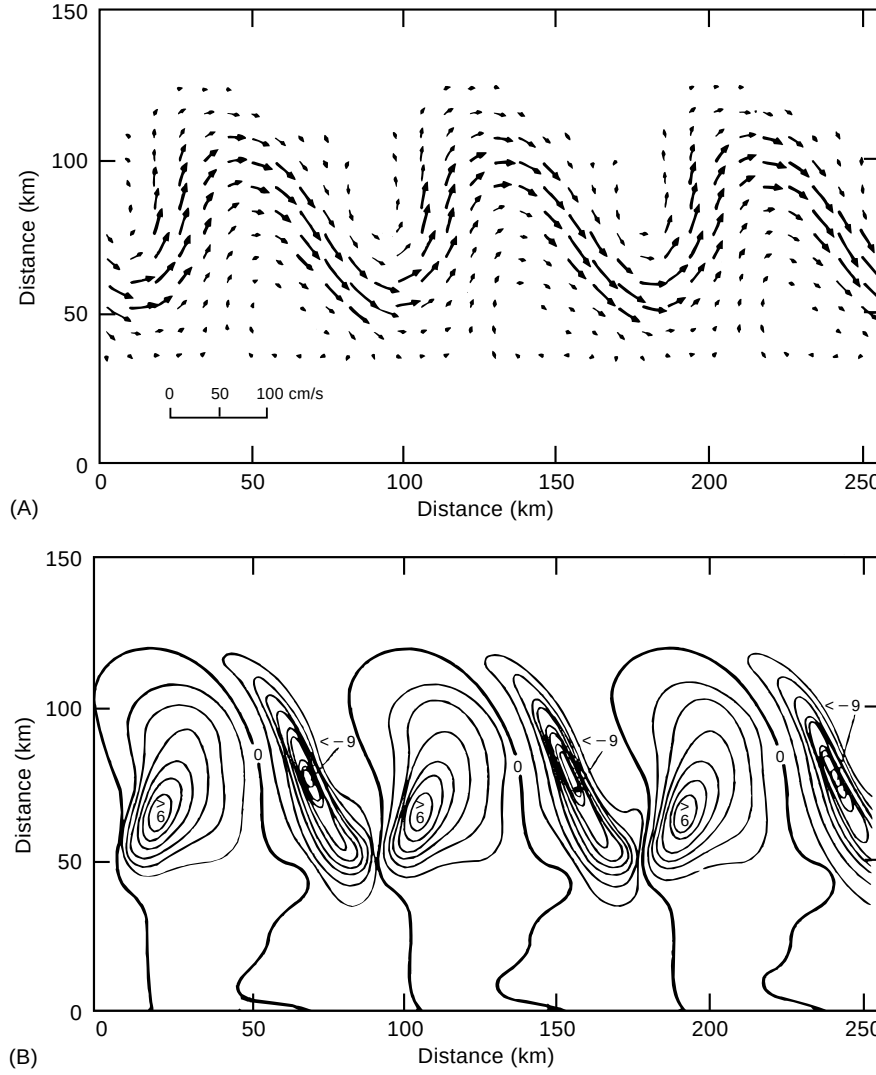

a0405fig0008 **Figure 8** Simulation of a meandering mesoscale jet: (A) velocity on an isopycnal surface with a mean depth of 20 m; (B) vertical velocity ($m\,d^{-1}$) on the same isopycnal surface as in (A). Note the consistent pattern of the vertical motion with respect to the structure of the jet. (Reproduced with permission from Woods JD (1988) Mesoscale upwelling and primary production. In: Rothschild BJ (ed) *Toward a Theory on Physical–biological Interactions in the World Ocean.* London: Kluwer Academic.)

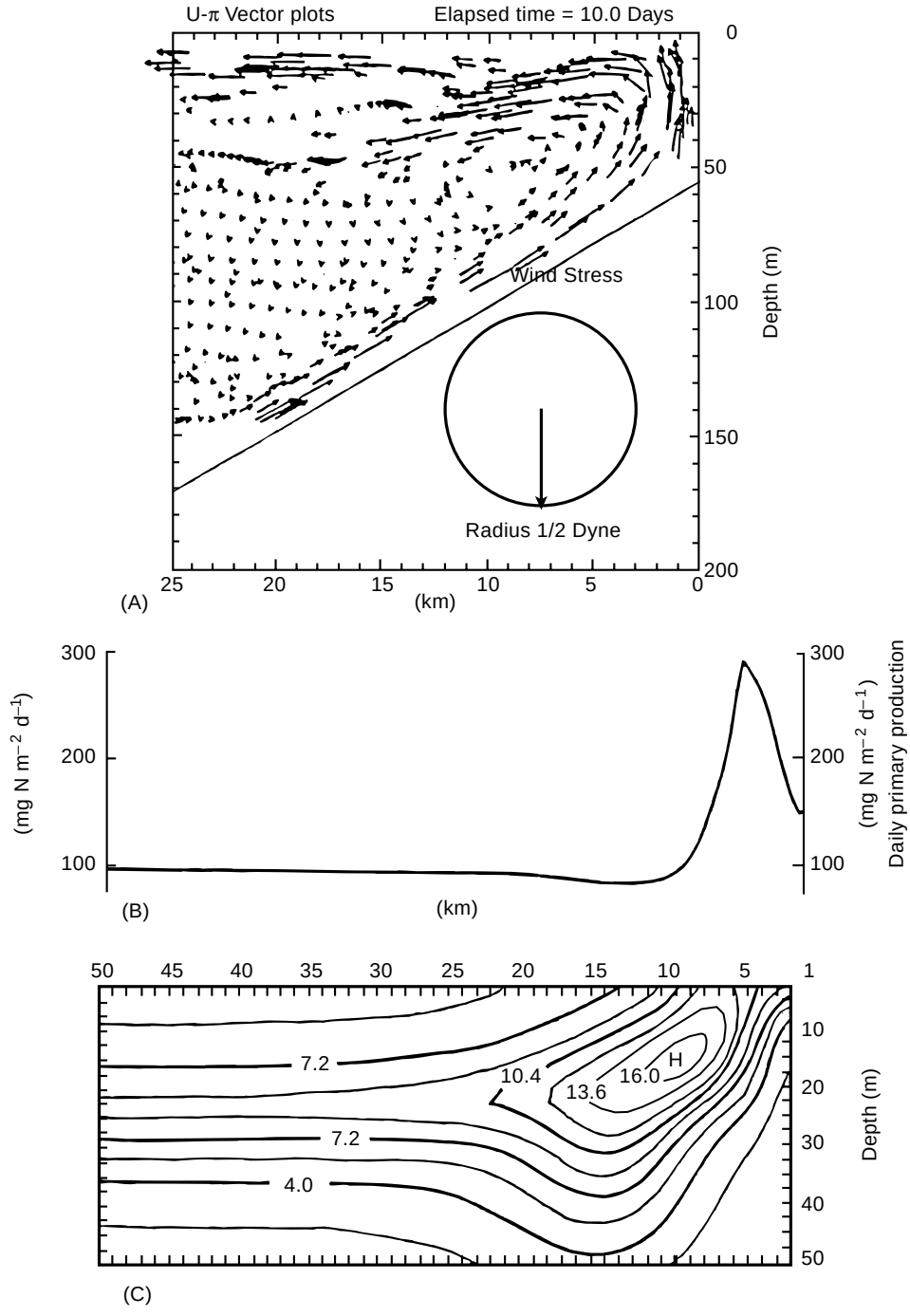

a0405fig0011 **Figure 11** Snapshot from a two-dimensional coupled model of coastal upwelling. (A) Circulation in the transverse plane normal to the coast (maximum horizontal and vertical velocities are -6.1 and $0.05\,\mathrm{cm\,s^{-1}}$, respectively); (B) daily gross primary production; (C) phytoplankton distribution (contour interval is $1.6\,\mu\mathrm{g}$ at $\mathrm{N\,l^{-1}}$. (Reproduced with permission from Wroblewski JS (1977) A model of plume formation during variable Oregon upwelling. *Journal of Marine Research* 35(2): 357–394.

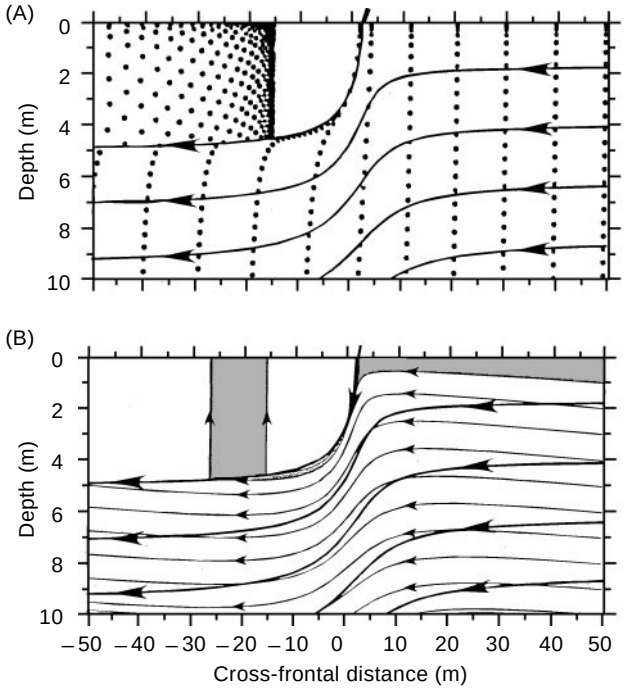

a0405fig0013 **Figure 13** Surface-seeking organisms aggregating at a propagating front. Modeled particle locations (dots, panel (A)) and particle streamlines (thin lines, panel (B)) in the cross-frontal flow. The front is centered at $x = 0$, and the coordinate system translates to the right with the motion of the front. Flow streamlines are represented in both panels as bold lines; they differ from particle streamlines due to propagation of the front. The shaded area in (B) indicates the region in which cells are focused into the frontal zone, forming a dense band at $x = -20$ m. Compare patterns in (A) and (B) with an aerial photograph of dense bands of *Lingulodinium polyedrum* populations associated with internal waves about 1 km off the coast of La Jolla. (Reproduced with permission from Franks, 1997.)